

# SCIENTIFIC REPORTS

OPEN

## AAV Gene Therapy for MPS1-associated Corneal Blindness

Melisa Vance<sup>1,\*</sup>, Telmo Llanga<sup>1,2,\*</sup>, Will Bennett<sup>1,2</sup>, Kenton Woodard<sup>1</sup>, Giridhar Murlidharan<sup>1,3</sup>, Neil Chungfat<sup>2</sup>, Aravind Asokan<sup>1,3</sup>, Brian Gilger<sup>5</sup>, Joanne Kurtzberg<sup>6</sup>, R. Jude Samulski<sup>1,4</sup> & Matthew L. Hirsch<sup>1,2</sup>

Received: 03 December 2015

Accepted: 01 February 2016

Published: 22 February 2016

Although cord blood transplantation has significantly extended the lifespan of mucopolysaccharidosis type 1 (MPS1) patients, over 95% manifest cornea clouding with about 50% progressing to blindness. As corneal transplants are met with high rejection rates in MPS1 children, there remains no treatment to prevent blindness or restore vision in MPS1 children. Since MPS1 is caused by mutations in *idua*, which encodes alpha-L-iduronidase, a gene addition strategy to prevent, and potentially reverse, MPS1-associated corneal blindness was investigated. Initially, a codon optimized *idua* cDNA expression cassette (opt-IDUA) was validated for IDUA production and function following adeno-associated virus (AAV) vector transduction of MPS1 patient fibroblasts. Then, an AAV serotype evaluation in human cornea explants identified an AAV8 and 9 chimeric capsid (8G9) as most efficient for transduction. AAV8G9-opt-IDUA administered to human corneas via intrastromal injection demonstrated widespread transduction, which included cells that naturally produce IDUA, and resulted in a >10-fold supraphysiological increase in IDUA activity. No significant apoptosis related to AAV vectors or IDUA was observed under any conditions in both human corneas and MPS1 patient fibroblasts. The collective preclinical data demonstrate safe and efficient IDUA delivery to human corneas, which may prevent and potentially reverse MPS1-associated cornea blindness.

Mucopolysaccharidosis 1 (MPS1) is an autosomal recessive lysosomal storage disorder caused by null or nonsense mutations in the gene encoding alpha-L-iduronidase (IDUA), a ubiquitous intracellular and secreted enzyme that breaks down glycosaminoglycans (GAGs). In the absence of functional IDUA, GAGs accumulate in lysosomes and disrupt the normal intracellular trafficking of lipids, sugars, and proteins causing multisystem end organ damage. The incidence of MPS1 is approximately 1 in 100,000 and the disease is characterized by hepatosplenomegaly, cardiac insufficiency, bone and joint deformities, dwarfism, mental retardation and serious nervous system problems, which commonly result in death by 10 years of age. Additional symptoms include hearing loss, joint stiffness, and clouding of the cornea which results in loss of vision<sup>1</sup>.

Current MPS1 treatments include IDUA enzyme replacement therapy (ERT) (Aldurazyme) via intravenous injections, which has proven useful in reducing hepatosplenomegaly, and in improving myocardial function, pulmonary symptoms and motility in MPS1 patients with mild disease. A more promising treatment relies on allogeneic hematopoietic stem cell transplantation (HSCT) which has been used for the past 2–3 decades in MPS1 patients. HSCT has proven successful at improving cognitive function, reducing hepatosplenomegaly, preventing ischemic cardiac disease and prolonging the patient's lifespan, in some cases by decades. Clinical outcomes are best when myeloablative chemotherapy and cord blood donors are utilized, as it increases the extent of sustained donor chimerism. A third MPS1 treatment approach that is still under preclinical evaluation relies on an adeno-associated virus (AAV) IDUA gene addition strategy. Central nervous system (CNS) targeted AAV-IDUA gene therapy has been explored in murine, feline, and canine MPS1 models following administration via several routes including the carotid artery, intraparenchymal, intraventricular and intrathecal<sup>2–4</sup>. These gene therapy studies independently report histological, biochemical, and in particular cognitive improvements while, importantly, IDUA-related toxicity was not observed. However, ERT, HSCT and AAV CNS-targeted or systemic gene

<sup>1</sup>Gene Therapy Center, University of North Carolina at Chapel Hill, NC, 27599, USA. <sup>2</sup>Department of Ophthalmology, University of North Carolina, Chapel Hill, NC, 27599, USA. <sup>3</sup>Department of Genetics, University of North Carolina, Chapel Hill, NC, 27599, USA. <sup>4</sup>Department of Pharmacology, University of North Carolina, Chapel Hill, NC, 27599, USA. <sup>5</sup>College of Veterinary Medicine, NCSU-CVM, Clinical Sciences, Raleigh, NC, USA. <sup>6</sup>Department of Pediatrics, Duke University, Durham, NC, 27710, USA. \*These authors contributed equally to this work. Correspondence and requests for materials should be addressed to M.L.H. (email: mhirsch@email.unc.edu)

therapy exhibit a common deficiency; the inability to correct MPS1-associated maladies in privileged compartments including the joint and eye.

Regarding the ocular abnormalities, approximately 90% of MPS1 children lose vision due to corneal clouding, which has been attributed to the abnormal presence of vacuolated stroma cells<sup>5</sup>. Detailed analyses of MPS1 human corneas demonstrated an accumulation of chondroitin and dermatan sulphate GAGs, which alter the uniform distribution, organization, and size of collagen fibrils<sup>6,7</sup>. Cornea transplantation in MPS1 children has been used to address the corneal blindness, however the high rejection rate has, in recent years, discouraged this treatment as standard practice. On the contrary, isolated reports using HSCT have demonstrated the capacity to stabilize, improve, and in some cases restore corneal clarity<sup>7–12</sup>. These data strongly support our hypothesis that cornea abnormalities can be prevented or reversed in the presence of IDUA<sup>8</sup>.

Cornea targeted AAV gene therapy has been investigated in animal models primarily following 2 routes of administration; topical applications in wound healing assays and direct injection to the corneal stroma. Regarding topical applications, AAV serotype 9 (AAV9) was reported most efficient for stromal transduction, however, this was nearly entirely localized to the epithelial/stromal boundary<sup>13</sup>. Regarding AAV gene delivery following intrastromal injection into human cornea explants, it was observed that AAV8 was more efficient than AAV2 or AAV1 for stromal transduction, which encompassed multiple cell types including CD34+ keratocytes and macrophages<sup>14</sup>. Importantly, both of these routes of drug administration observed no deleterious consequences related to the AAV vector<sup>13–15</sup>.

The purpose of the present study is to explore AAV-mediated IDUA delivery as an effective treatment for MPS1 cornea clouding. Towards this end, we engineered an AAV vector cassette that efficiently restores IDUA to MPS1 patient fibroblasts in a dose-dependent manner. Normal, and supraphysiological, IDUA activity was demonstrated in both cellular lysates and in culture supernatants. Then, as MPS1 corneal disease has been attributed to stroma abnormalities<sup>5</sup>, the AAV serotypes reported most efficient for stromal transduction were evaluated in human corneas. The results demonstrate efficient transduction (AAV9 > AAV8), however, an AAV8/9 chimeric (8G9) capsid performed significantly better than either parental serotype. Using AAV8G9, IDUA was over-produced in the human corneal stroma with widespread distribution in multiple cell types, which included cells that naturally produce IDUA. Functional assays in human corneas demonstrated a 10-fold elevation of IDUA activity seven days post-injection without any indications of toxicity. Given the popularity of AAV gene therapy in ocular clinical trials, the soluble nature of IDUA, and the potential for compassionate use of AAV-IDUA in MPS1 children, our preclinical data herein provides encouraging results for a potential treatment of MPS1-associated corneal clouding.

## Results

To develop an AAV IDUA expression cassette, the human *idua* cDNA (NM\_000203) was codon optimized for human production (opt-IDUA) and situated between the CMV promoter and the SV40 poly-adenylation sequence in an AAV inverted terminal repeat serotype 2 plasmid context (Fig. 1A). Production of IDUA protein by the pTR-CMV-opt-IDUA plasmid was confirmed, after performing transfection and Western Blot experiments with human embryonic kidney 293 cells and MPS1 patient fibroblasts (Fig. S1A,B). Additionally, IDUA protein levels from the codon optimized open reading frame were similar to that generated by wild type IDUA cDNA in both 293 cells and MPS1 patient fibroblasts (Fig. S1).

AAV2-opt-IDUA vectors were prepared as described<sup>16</sup> and used for characterization in MPS1 patient derived fibroblasts. Immortalized normal human fibroblasts (NHF) served as the control cell line<sup>17</sup>. In dose escalation experiments, AAV2-opt-IDUA transduction of MPS1 fibroblasts resulted in increasing levels of IDUA restoration, in both cellular lysates and in the culture supernatant (Fig. 1B). In fact, as resting levels of IDUA in NHF are relatively low, a dose of 5,000 viral genomes/cell resulted in already supraphysiological levels in both cell lysates and in culture supernatants (Fig. 1B). Consistently, IDUA function was restored and elevated in transduced MPS1 patient fibroblasts with a 10-fold and 30-fold increases in cellular lysate and supernatant, respectively, at the highest investigated dose (Fig. 1C,D). Despite IDUA overproduction following AAV vector transduction, no toxicity was observed in patient fibroblasts at any dose using a dye exclusion assay (Fig. S2). Importantly, these results demonstrate the functionality and safety of AAV2-opt-IDUA in a MPS1 patient context.

An analysis of MPS1 patient corneas attributed stromal abnormalities as the cause of the corneal opacity that results in vision loss<sup>5</sup>. Therefore, direct administration of AAV-opt-IDUA should restore IDUA activity in the corneal stroma compartment of MPS1 patients, hopefully preventing or reversing the MPS1 phenotype. Previous reports demonstrated the utility of both AAV8<sup>14</sup> and AAV9<sup>13</sup> for human keratocyte transduction, one of the most prevalent cell types present in the cornea. As such, these capsids, carrying a self-complementary (sc) AAV-CMV-GFP genome, were evaluated in normal human corneal explants, which remain viable for weeks post-mortem. Preliminary experiments demonstrated that a volume of 50µl injected into the stroma was tolerated with minimal tissue distension and a distribution across ≈50% of the adult cornea using the vector vehicle containing india ink (Fig. S3). Therefore, AAV serotypes 8 or 9 containing a GFP reporter gene were administered to human cornea stroma by injection (1e<sup>10</sup> vg in 50 µl) and analyzed seven days later by Western blotting. Given the reports of both 8 and 9 for cornea transduction, an AAV8/9 chimeric capsid (8G9), containing the galactose receptor of AAV9 engrafted on the AAV8 capsid was also investigated in the same manner<sup>13,14</sup>. Western blotting suggested that AAV8G9-GFP resulted in greater transduction than either parent serotype (Fig. 2A). In order to quantify the degree of viral transduction of the different serotypes on the human corneas, we performed a quantitative ELISA GFP assay (Fig. 2B). Single stranded versions of the AAV serotypes 8, 9 and 8G9 carrying the CMV-GFP cassette were used for cornea infection for seven days. After that time, viral transduction was determined according to the amount of GFP expressed by the infected cells. Statistical analysis revealed that AAV8G9 was able to infect the human cornea to a higher extent, compared to the transduction obtained by the parental

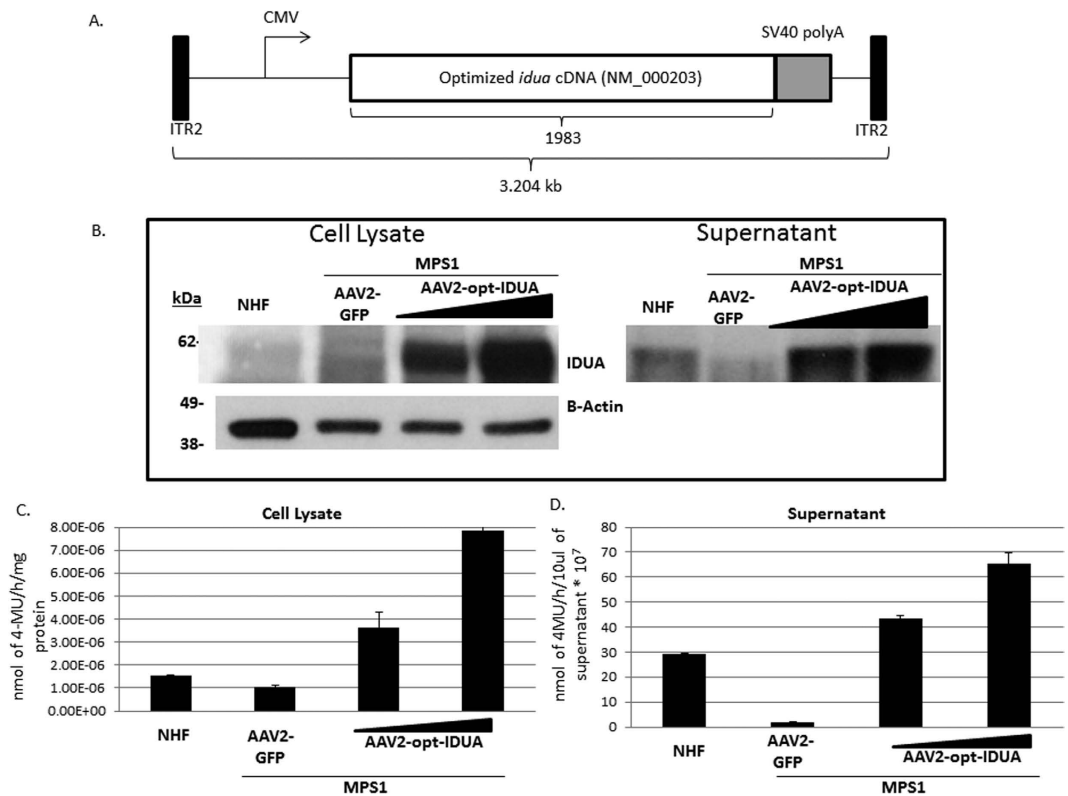


**Figure 1. Restoration of IDUA activity in MPS1 patient fibroblasts by AAV gene therapy.** (A) Schematic diagram of the AAV-IDUA optimized vector construct. (B) Cell lysates (Left panel) and supernatants (Right panel) from AAV2 infected and not-infected fibroblasts, normal human fibroblasts (NHF) or MPS1 fibroblasts, were analyzed for IDUA protein expression. Detection of  $\beta$ -actin was performed as a loading control of total protein in cell lysates. All the experiments were performed in triplicate. (C) Functional activity of IDUA protein was obtained for cell lysates and supernatants from AAV2 infected and not-infected fibroblasts, NHF or MPS1 fibroblasts. For cell lysates, the nmoles of 4-MU were normalized to one hour reaction and mg total protein. For cell supernatants, the nmoles of 5-MU were normalized to 10  $\mu$ l of the sample. All the experiments were performed in triplicate. 4-MU, 4-methylumbelliferone; CMV, cytomegalovirus promoter; ITR, inverted terminal repeats; GFP, Green fluorescence protein.

capsids AAV8 or AAV9;  $p \leq 0.05$  for both cases. This analysis was performed with a total of five human corneas of mixed gender.

In order to determine the biodistribution of single-strand AAV8G9-GFP transduction (final volume 50  $\mu$ l), GFP immunofluorescence was performed on human corneal cross sections. The results demonstrate a lateral spread of vector transduction across the cornea with penetration into the deeper stromal layers, including some endothelial cell transduction (Fig. 2C). Co-staining with CD34, a marker of keratocytes, with alpha-smooth muscle actin (alpha-SM), indicative of differentiated keratocytes, and with F4/80, a macrophage marker, demonstrated the corneal cell promiscuity for the AAV8G9 capsid (Fig. 2D).

Following confirmation that the AAV8G9 capsid was the most efficient for corneal stroma transduction, we determined if the cell types transduced by AAV8G9 naturally produce IDUA. To do this, dual staining for the cell type marker and the IDUA protein was performed in normal untreated human corneas. The results indicate that all of the confirmed corneal cell types transduced by AAV8G9 naturally produce IDUA (Fig. 3A).

Next, AAV8G9-opt-IDUA preclinical vector preparations were produced by the UNC Vector Core and evaluated in normal human corneas *ex vivo*. For these experiments, injection of single-strand AAV8G9-GFP was evaluated and PBS served as the negative control. Seven days post-injection ( $1 \times 10^{10}$  vg in 50  $\mu$ l), total protein was recovered and IDUA abundance was investigated by Western blotting. In whole corneal lysates, it was observed that the resting levels of IDUA are relatively low and that vector-derived IDUA, both the precursor and cleaved forms, was readily detected (Fig. 3B). Consistently, a 10-fold elevation of IDUA activity was observed in the AAV8G9-opt-IDUA injected corneas when compared to the normal levels found in human corneas (Fig. 3C).

By immunofluorescence staining and detection on human cornea cross sections, the resting levels and distribution of IDUA were determined (Fig. 4). As MPS1 patient corneas are rare, staining under the same conditions but without the IDUA primary antibody served as the negative control. The results demonstrate relatively low levels of IDUA within the corneal stroma that were also present in the corneal epithelia and to a lesser extent, in the endothelial cell layer (Fig. 4). IDUA staining was also performed on human cornea cross sections that were injected with AAV8G9-opt-IDUA. The results correlate to those of the IDUA Western blot and the functional

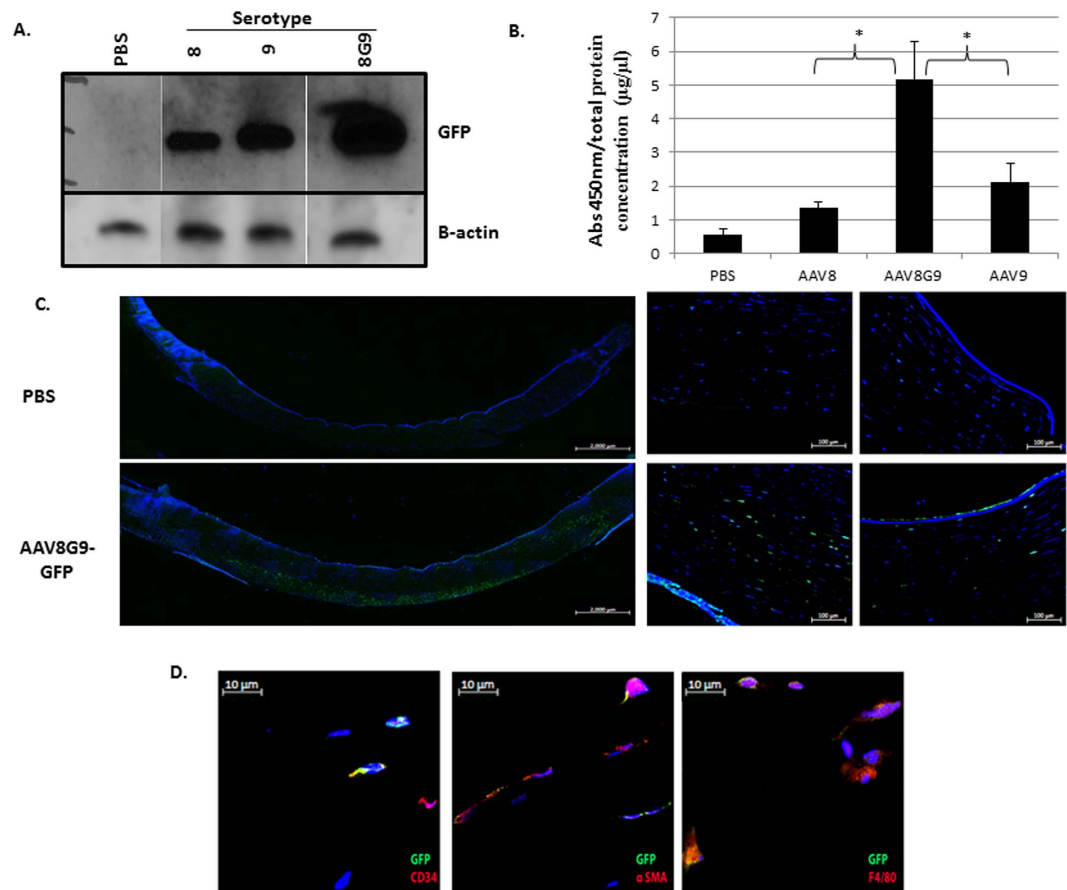


**Figure 2. AAV capsid serotype evaluation in human cornea.** (A) Human corneas were injected with a self-complementary CMV-GFP cassette encapsidated in AAV serotypes 8, 9, or the 8/9 chimeric 8G9. Seven days later Western blot was used to detect GFP. PBS corresponds to a human cornea injected with only PBS (vehicle control). Detection of  $\beta$ -actin was performed as a loading control. (B) Human cornea pieces were incubated with  $1 \times 10^{10}$  viral genomes of each serotype: 8, 9, or the chimeric 8G9, but as single stranded viruses. Seven days following viral infection, the tissues were collected and the protein lysates were obtained for quantification of GFP. Human corneas incubated with the medium but replacing the viral addition for PBS were used as negative controls (PBS). Absorbance measurements at 450nm were normalized to total protein concentration. (\*corresponds to  $p \leq 0.05$  when performing T-tests comparing normalized absorbance 450nm values for AAV8G9 with AAV8 or AAV9;  $N = 5$ ). (C) Single-strand AAV8G9-CMV-GFP was injected into the stroma of human corneas and harvested for histology 7 days later. Left- Immunofluorescence image showing the distribution of recombinant AAV8G9-GFP transduction across a human cornea section. Human corneas injected with PBS served as the negative control. Images were obtained with  $10\times$  objective and assembled by stitch processing. The scale bar is equal to  $2000 \mu\text{m}$ . Right- Different areas of the same stained human cornea taken with  $20\times$  objective. The scale bar is equal to  $100 \mu\text{m}$ . Hoechst was used for nuclei counterstain. (D) A representative section of the corneas in (C) stained with GFP (green) and the indicated cell marker (red). The scale bar is equal to  $10 \mu\text{m}$ . Hoechst was used for nuclei counterstain.

assay (Fig. 3) in that there is an approximate 5–10 fold increase in IDUA in normal human corneas treated with AAV8G9-opt-IDUA compared to the resting level in human corneas (Fig. 4). Furthermore, similar to the results observed with AAV8G9-GFP, vector derived IDUA appeared well distributed (Figs. 2C and 4).

Considering restoration of IDUA to the MPS1 patient cornea, it is critical to determine any vector or IDUA related toxicity. Due to unavailability of a small animal model for MPS1 that develops cornea clouding, we performed apoptosis experiments in normal human corneas following AAV8G9-GFP or AAV8G9-opt-IDUA stromal injection ( $1e^{10}$  vg). TUNEL staining, which detects fragmented DNA indicative of cellular apoptosis, was performed on day 7 post-injection. Although the nuclease-treated positive control samples demonstrated extensive TUNEL staining, the staining of corneas in which IDUA abundance/function were significantly elevated did not show a significant difference to the ones non-injected or injected with AAV8G9-GFP (Fig. 5). These results are consistent with those obtained using MPS1 patient fibroblasts and collectively suggest the safety of AAV8G9-opt-IDUA gene therapy in MPS1 patient corneas. However, a complete toxicity study should be performed in an *in vivo* MPS1 model, where immune responses and/or liver toxicity could be evidenced.

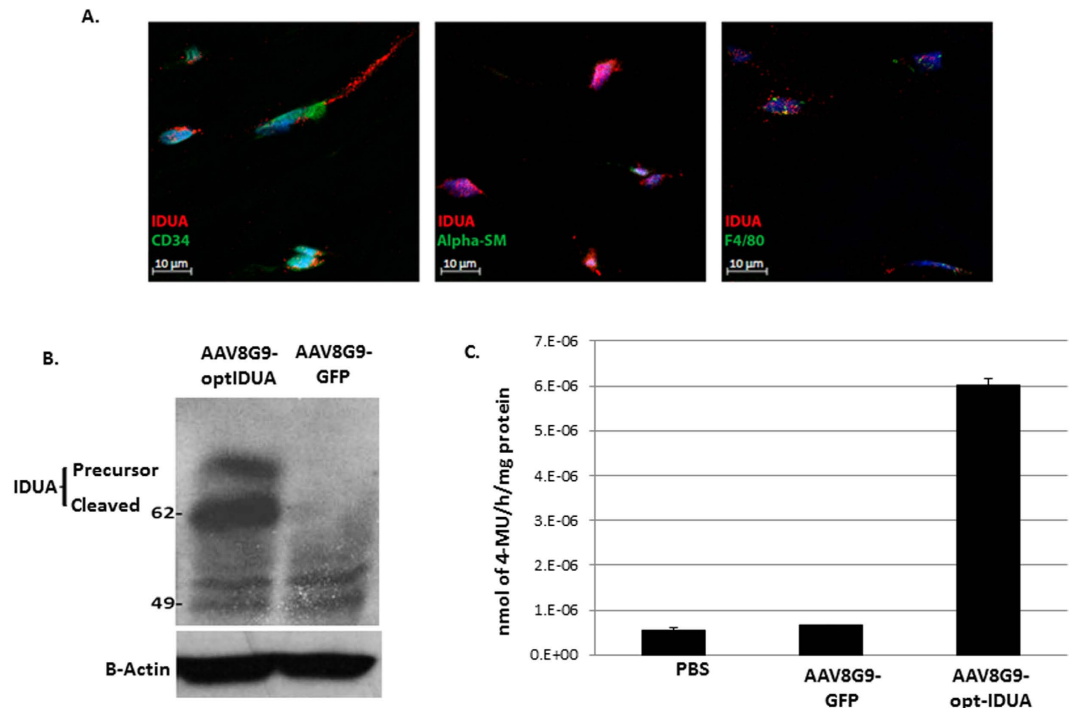


**Figure 3. Restoration of IDUA activity in human corneas by AAV8G9-opt-IDUA.** (A) A representative section of a normal non-injected cornea stained with IDUA antibody (red) and a cell marker (green). Hoechst was used for nuclei counterstain. The scale bar is equal to 10  $\mu$ m. (B) Western blot detecting IDUA amounts produced after injection of AAV8G9-opt-IDUA. Administration of AAV8G9-GFP served as a vector infection control. B-actin serves as a loading control. (C) Functional activity of IDUA protein obtained from human corneas 7 days post-injection of AAV8G9-opt-IDUA. AAV8G9-GFP served as the negative control. The nmoles of 4-MU were normalized to one hour reaction and mg total protein. PBS corresponds to a human cornea injected with only the vehicle control. The experiment was performed in triplicate.

## Discussion

Hematopoietic stem cell transplantation, after myeloablative chemotherapy using allogeneic bone marrow or umbilical cord blood donors has been shown to extend life and improve its overall quality, particularly when performed in MPS1 children under 2 years of age<sup>18–22</sup>. Engrafted donor cells provide a source of systemic IDUA and, through engraftment of donor microglial cells, enzyme replacement in the brain. Transplanted children, surviving 1–2 decades after HSCT with full donor chimerism, have normal blood IDUA levels with normal, to near normal, cognitive and cardiac functions. Later, and ongoing, manifestations of MPS1 after transplantation do occur and generally are limited to the joints, bones, and the eye, all of which are organs with lower perfusion and lower delivery of donor-derived IDUA. As such, our preclinical corneal approach explored herein, was designed as a supplemental MPS1 therapy to address the shortcomings of stem cell transplantation and AAV gene therapy targeting the CNS.

As MPS1 patient corneas are rarely available, we initially investigated disease correction in MPS1 patient fibroblasts. The data demonstrate restoration of IDUA function using a low vector dose. This is, in part, due to the relatively low level of IDUA in normal fibroblasts which is presumably sufficient for normal cellular physiology (Fig. 1). Consistently, the abundance of IDUA found in normal human corneas was also modest. In fact, in whole cornea lysates, IDUA abundance by Western blotting was not readily detected, however, tissue histology identified resting levels of IDUA in corneal epithelia, endothelia and the majority in multiple cell types found in the stroma (Figs 3 and 4). This evaluation of IDUA abundance and AAV-mediated restoration highlights a very important aspect to our corneal gene therapy approach: mainly that only a low amount of IDUA is necessary to restore WT IDUA function in the corneas of MPS1 children. This evidence is supported by studies with the MPS1 canine model, in which cornea clouding was significantly improved in presence of low levels of IDUA, meanwhile higher levels of IDUA did not provide further benefit<sup>23</sup>. In our experiments, our chosen AAV dose in the cornea explants ( $1 \times 10^{10}$  vg) was found to be excessive and resulted in a 10-fold supraphysiological elevation of IDUA function. However, even at this high IDUA level no apoptosis was detected (Figs 3–5). Given the ability of secreted IDUA to cross-correct neighboring cells, the low resting levels in normal human corneas, and the efficiency of AAV8G9-opt-IDUA for human cornea transduction, the data herein suggest that a low vector dose will result in normal levels of IDUA in MPS1 patient corneas. Furthermore, reported complications associated with a neutralizing antibody response to the IDUA transgene product (IDUA) are not anticipated as there are no antibodies in the human cornea<sup>24</sup>. However, at this point we are not able to predict the occurrence of any type of immune reaction or liver-associated toxicity.

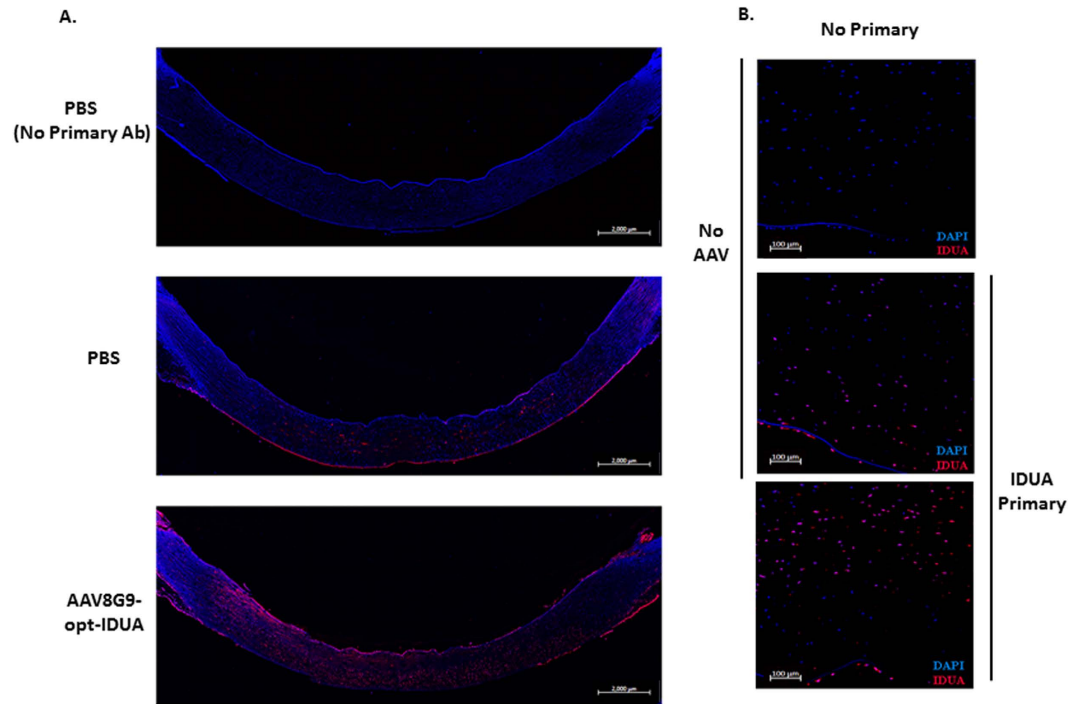


**Figure 4. Distribution of IDUA protein following AAV-8G9-opt-IDUA transduction.** (A) Immunofluorescence image showing the distribution of IDUA protein across a human cornea section seven days post-injection of AAV8G9-opt-IDUA or PBS (vehicle). The images were obtained with 10 $\times$  objective and assembled by stitch processing. The scale bar is equal to 2000  $\mu$ m. Hoechst was used for nuclei counterstain. (B) Cross section of the same stained human corneas but taken with a 20 $\times$  objective. The top figure corresponds to the negative control of staining, which was treated in the same manner as the other samples but without the primary antibody. Hoechst was used for nuclei counterstain. The scale bar is equal to 100  $\mu$ m. The experiment was performed in duplicate.

Given the collective data herein, restoring IDUA function in MPS1 corneas seems quite feasible. Furthermore, it appears that AAV8G9 elicits IDUA production in stromal cells that naturally produce IDUA, as well as in the endothelial layer (Fig. 4). Despite the ability to restore IDUA in the cornea, the question of whether or not restoration of IDUA in the cornea will reverse corneal clouding remains unanswered. However, several lines of evidence suggest that IDUA in the MPS1 cornea will reverse the corneal blindness<sup>7,23</sup>. In particular, the reduction of corneal opacity, but not complete correction, was reported in MPS1 patients receiving HSCT<sup>5</sup>. In that work it was hypothesized that the partial correction was due to restoration of IDUA in the corneal endothelium but not in the stroma. As our AAV-opt-IDUA strategy is capable of transducing both of these compartments (Fig. 4), the likelihood of reversing or preventing MPS1-associated corneal blindness, as a supplemental therapy to HSCT or AAV systemic gene delivery remains a viable possibility.

## Materials and Methods

**Production of AAV vectors.** For cell culture experiments, a previously described triple transfection method was used to generate the vectors used herein<sup>25</sup>. This method used the pXR2 or pXR8G9 (manuscript submitted) plasmids, which all contain *rep2* of AAV and individually the capsid genes of the indicated serotype. The plasmid containing the intended AAV genome was first constructed by substituting the *egfp* gene in pTR-CMV-eGFP with the codon optimized IDUA cDNA (provided by GenScript) at the AgeI and SalI sites (now called pTR-CMV-opt-IDUA), or the wild type full-length hIDUA cDNA (kindly provided by Dr. Aronovich<sup>26</sup>) (now called pTR-CMV-wt-IDUA). Following AAV production and cesium chloride gradient separation<sup>25</sup>, peak fractions were dialyzed against PBS, and titered by quantitative PCR (CMV\_F CAA GTA CGC CCC CTA TTG AC, CMV\_R AAG TCC CGT TGA TTT TGG TG) which was confirmed by Southern dot blot<sup>25</sup>. For the experiments in human explants, GMP grade vector preparations were provided by the UNC vector core.

**Cell culture and vector transduction.** Human embryonic kidney 293 cells, MPS1 patient fibroblasts, and normal human fibroblasts<sup>17</sup> were maintained at 37  $^{\circ}$ C in a 5% CO<sub>2</sub> atmosphere in Dulbecco's modified Eagle's medium (Sigma) supplemented with 10% fetal bovine serum and penicillin-streptomycin (100 U/ml). Transduction of cultured cells was performed in a 24 well plate in a fixed volume. For these experiments, vector was added to the wells at the indicated viral genome per cell dose and was not removed for the duration of the experiment.

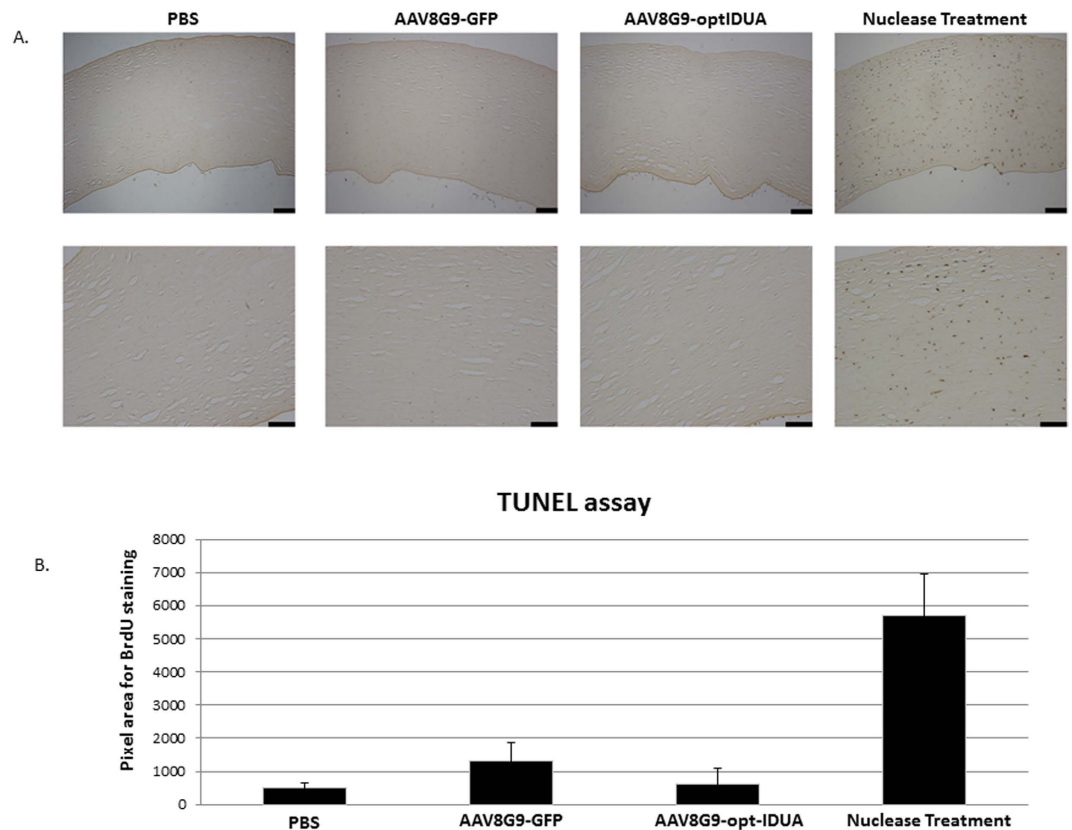


**Figure 5. No apoptosis following AAV8G9-opt-IDUA injection in human corneas.** (A) Human corneas injected with PBS, AAV8G9-GFP, or AAV8G9-opt-IDUA were processed 7 days later for TUNEL staining. Top, images taken at  $10\times$ . Bottom, images taken at  $20\times$ . As a positive control, human corneas injected with PBS where nuclease treated. The scale bar is equal to  $100\mu\text{m}$ . (B) Quantitation of pixel area for total staining performed in (A). A minimum of 7 areas per cornea for each treatment were counted using SigmaScan Pro software. No statistical difference between cytotoxicity for corneas injected with AAV8G9-GFP or AAV8G9-opt-IDUA was observed ( $p > 0.05$ ).

**Human Cornea Experiments.** All experimental protocols were approved by the University of North Carolina at Chapel Hill. Human corneas were provided by the miracles in sight tissue procurement bank. These unidentified post-mortem tissue experiments were performed in accordance with the human subjects research office of human research ethics at the University of North Carolina at Chapel Hill (IRB-14-1019). The corneas of both genders were maintained in the supplied opti-mem at  $37^\circ\text{C}$  in a  $5\% \text{CO}_2$  atmosphere. Injections were performed with a 31 gauge insulin syringe. India ink was used as a dye to verify the injections. Corneas were then cultured for 7 days and analyzed as described in the text. For detection of GFP by Elisa, human corneas were trimmed into several pieces of similar size and each piece was incubated in a separate well in a certain condition.

**Quantitative GFP detection by ELISA.** Human cornea pieces were infected with  $1 \times 10^{10}$  viral genomes of each serotype: 8, 9, or the 8/9 chimeric 8G9 for seven days. Cell lysates were obtained by cutting each cornea into pieces and incubating the pieces with  $200\mu\text{l}$  M-PER<sup>®</sup> Mammalian Protein Extraction Reagent (Pierce, catalog number: 78503) and  $2\mu\text{l}$  Halt<sup>™</sup> Protease Inhibitor Cocktail for 10 minutes, followed by repeating freezing and thawing procedures. An aliquot of  $100\mu\text{l}$  of each lysate was incubated at  $4^\circ\text{C}$  overnight with the anti-GFP antibody coated plate (Cell Biolabs, Inc, catalog number AKR-121). Following extensive washes, a second incubation with an anti-GFP antibody, but this time biotinylated, was performed for 2 hours at room temperature. Wells were washed and streptavidin-enzyme conjugate was added to each well. The reaction took place by adding the substrate for the enzyme and once the color was developed, the reaction was stopped and absorbance at  $450\text{nm}$  was measured.

**Functional IDUA assay.** Quantitative IDUA enzyme activities were measured as previously described<sup>27</sup>. Briefly,  $10\mu\text{l}$  of a supernatant or cell lysis solution, obtained the same way as for the detection of GFP by ELISA, were incubated with  $50\mu\text{M}$  4-methylumbelliferyl alpha-L-iduronide made in  $0.4\text{M}$  sodium formate buffer, pH 3.5, containing  $0.2\%$  Triton x-100 at  $37^\circ\text{C}$  for 60 min in the dark. Reactions were stopped by adding  $80\mu\text{l}$  of  $0.5\text{M}$  NaOH/glycine buffer pH 10.3. The 96 well plates were centrifuged for 1 min  $13000\text{rpm}$  at  $4^\circ\text{C}$  and supernatants were transferred to a black 96w plate, clear bottom with lid for measuring fluorescence at  $450\text{nm}$ , following excitation at  $365\text{nm}$ . The amount of cleaved substrate was calculated from a standard curve, previously established

with 4-methylumbelliferone and expressed as nmol/h/mg for enzyme activity in cell lysates, or nmol/h/10  $\mu$ l for analysis of supernatants. The protein amount for each sample was determined with the BCA assay (Pierce™ BCA Protein Assay Kit, catalog number: 23225).

**Tunel Assay.** Apoptotic cells generated due to the cellular cytotoxicity during AAV infection of human cornea explants were determined by deoxynucleotidyltransferase (TdT)-mediated dUTP-biotin nick end labeling with DAB. Tunel assay was performed with TACS2 TdT-Blue Label *in situ* apoptosis detection kit (Trevigen, Gaithersburg, Md.). Briefly, following deparaffinization and rehydration, the human cornea sections were digested for 20 min in proteinase K. Slides were washed with 1  $\times$  PBS and the endogenous peroxidase activity was quenched by incubating the tissues with 3% H<sub>2</sub>O<sub>2</sub> solution in Methanol. After washing the slides with 1  $\times$  PBS, tissue sections were incubated with 1  $\times$  TdT labeling buffer for 5 min. The labeling reaction consisting of incubating the cornea tissues with TdT enzyme, dNTPs with biotinylated dUTP, and 1  $\times$  manganese chloride in 1  $\times$  TdT labeling buffer for 1 h in a humidified chamber at 37°C. The reaction was completed by incubating with 1  $\times$  TdT stop buffer. The fragmented DNA was visualized by treating the sections with streptavidin-conjugated horseradish peroxidase and DAB solution.

**Immunofluorescence Staining.** Human cornea tissues were embedded in paraffin and sectioned at a thickness of 5  $\mu$ m using a microtome. In order to stain the slide with immunofluorescence antibodies, sections were deparaffinized by incubating the slides in xylene for 5 min, two times total, followed by rehydration by immersing them sequentially in 100%, 95% and 70% ethanol solutions, 5 min each, and finally in water for 5 min. Before staining the sections, antigen retrieval procedure was performed in order to guarantee the exposure of epitopes, which were previously masked due to the paraffin embedding process. Specifically, slides were immersed into pre-heated antigen retrieval solution (Dako) at 98°C for 7 min. Non-specific binding sites within the tissues were then blocked by incubating the slides with 10% NGS, in 1  $\times$  PBS for 1 hour at RT. Slides were washed twice for 5 minutes each with 2% NGS in 1  $\times$  PBS. Sections were then incubated overnight at 4°C with primary antibody diluted appropriately in a solution consisting of 2% NGS in 1  $\times$  PBS. After incubation with primary antibody, slides were washed three times, for 5 minutes each, in order to remove non-specifically bound primary antibody. The washing solution contained 2% NGS in 1  $\times$  PBS. An appropriate fluorescently-labeled secondary antibody (5  $\mu$ g/ml) was then added to the slides diluted in 2% NGS in 1  $\times$  PBS, and slides were incubated for 1 hour at 4°C. Finally, slides were washed twice with 2% NGS in 1  $\times$  PBS three times, for five minutes each, followed by a last wash with 1  $\times$  PBS at 4°C. A couple of drops of Hoechst (Molecular probes- Life technologies, H3569 Hoechst 33258, Pentahydrate-1  $\mu$ g/mL) were added for 7 minutes to counterstain the nuclei within the section, followed by a wash with water. Slides were then coverslipped with Cytoseal 60 (Thermo Fisher Scientific (NYSE: TMO)).

**Primary antibodies used for this study.** For IDUA staining, Rabbit Polyclonal IDUA antibody (Biorbyt, catalog number: orb157615, dilution 1/50); for GFP staining, Chicken anti GFP antibody (Aves, catalog number: GFP-1020, dilution 1/100); for CD34 staining, mouse monoclonal antibody (clone: B-6) (Santa Cruz, sc-74499, dilution 1/100), for  $\alpha$ -Smooth Muscle Actin staining, mouse monoclonal antibody (R&D, clone #1A4, catalog number MAB1420, dilution 1/100), and for F4/80 marker staining, rat monoclonal antibody, (clone: BM8) (Santa Cruz, sc-52664, dilution 1/100). Secondary antibodies were the following: Alexa Fluor® 594 goat anti-rabbit IgG (A-11012) (Gibco – Invitrogen, Carlsbad, CA), Alexa Fluor® 594 goat anti-chicken IgG (A-11039) (Gibco – Invitrogen, Carlsbad, CA), Alexa Fluor® 594 goat anti-rat IgG (A-11006) (Gibco – Invitrogen, Carlsbad, CA) and Alexa Fluor® 488 goat anti-mouse IgG (A-11001) (Gibco – Invitrogen, Carlsbad, CA). Images from each slide were taken using a Zeiss LSM 780 Confocal Microscope with a 40 $\times$  objective (Olympus, Tokyo, Japan). Images that comprised the complete human cornea were taken with 10 $\times$  objective, the title function and then stitched. Images were then processed using Adobe Photoshop. Sections from each tissue were stained with secondary antibody alone as negative control staining in all experiments.

**MPS1 Cell Transfection and Western Blot.** MPS1 fibroblast patient cells were plated onto a 24 well plate at 20,000 cells per well. After 24 hours, nine wells were transfected for each treatment adding a mix 1  $\mu$ g of plasmid DNA, 3  $\mu$ l of PEI and 60  $\mu$ l of DMEM to each well. 24 hours after transfection, 40  $\mu$ l of supernatant were collected from each well and 3 wells were combined to form each sample. 40  $\mu$ l of DMEM were added to each well to maintain the same volume for later supernatant collections. 48 hours after transfection, total supernatant was collected combining 3 wells to again form triplicates. At that time total cell protein was harvested by adding 70  $\mu$ l of Mammalian Protein extraction Reagent (Thermo Scientific Cat: 78501), per well and following reagent protocol.

For Western blot, Protein lysate was added to a solution of 5% beta-mercapto-ethanol in 4 $\times$  Nupage sample buffer. The resulting solution was boiled for 10 minutes and chilled on ice for 10 minutes and then run in a 10% Bis-tris pre-cast gel. Gel was run in 1  $\times$  MOPS running buffer, and transferred to a nitrocellulose membrane. The membrane was blocked with 5% milk in ddH<sub>2</sub>O, and probed with mouse host IDUA antibody (R&D Systems MAB-4119) for 2 hours at 1:500 dilution in PBS-Tween solution (0.5% Tween 20 in 1  $\times$  PBS) or mouse host beta-actin antibody (Sigma) at 1:5000 dilution in PBS-Tween. This was followed by mouse horse radish peroxide secondary antibody at 1:10000 dilution in PBS-Tween. Western-Bright Sirius chemi-luminescence reagent was used according to product protocol and blots were exposed using autoradiography film.

**Cell Transfection comparison of wild-type against codon optimized IDUA.** 293 cells were plated onto a 24 well plate at 100,000 cells per well. After 24 hours, 3 wells were transfected using a mix of 1  $\mu$ g of plasmid DNA, 3  $\mu$ l of PEI and 60  $\mu$ l of DMEM per well. Total cell protein was harvested after 72 hours by adding 70  $\mu$ l of Mammalian Protein extraction Reagent (Thermo Scientific Cat: 78501), to each well after saving the cell culture supernatant.



**MPS1 Patient Cell Toxicity Assay.** Patient Cells were plated onto a 24 well plate at 20,000 cells per well. AAV2-opt-IDUA was added after 24 hours in treatments of 5,000 and 50,000 viral genomes per cell with a total of eight replicates per treatment. After 72 hours, each well's supernatant was saved. This was followed by cell resuspension using 150  $\mu$ l of 0.05% trypsin. Trypsin was deactivated by adding back the respective supernatant to each well. All samples were analyzed using a Beckman Vi-cell XR cell viability dye exclusion analyzer.

## References

1. Aldenhoven, M. *et al.* Long-term outcome of Hurler syndrome patients after hematopoietic cell transplantation: an international multicenter study. *Blood* **125**(13), p. 2164–72 (2015).
2. Janson, C. G. *et al.* Comparison of Endovascular and Intraventricular Gene Therapy With Adeno-Associated Virus- $\alpha$ -L-Iduronidase for Hurler Disease. *Neurosurgery* **74**(1), p. 99–111 (2014).
3. Wolf, D. A. *et al.* Direct gene transfer to the CNS prevents emergence of neurologic disease in a murine model of mucopolysaccharidosis type I. *Neurobiol Dis* **43**(1), p. 123–33 (2011).
4. Hinderer, C. *et al.* Intrathecal gene therapy corrects CNS pathology in a feline model of mucopolysaccharidosis I. *Mol Ther* **22**(12), p. 2018–27 (2014).
5. Huang, Y. *et al.* Ultrastructural study of the cornea in a bone marrow-transplanted Hurler syndrome patient. *Exp Eye Res* **62**(4), p. 377–87 (1996).
6. Alroy, J., M. Haskins & D. E. Birk, Altered corneal stromal matrix organization is associated with mucopolysaccharidosis I, III and VI. *Exp Eye Res* **68**(5), p. 523–30 (1999).
7. Fahnehjelm, K. T. *et al.* Ocular findings in four children with mucopolysaccharidosis I-Hurler (MPS I-H) treated early with haematopoietic stem cell transplantation. *Acta Ophthalmol Scand* **84**(6), p. 781–5 (2006).
8. Hobbs, J. R., Bone marrow transplantation for inborn errors. *Lancet* **2**(8249), p. 735–9 (1981).
9. Hoogerbrugge, P. M. *et al.* Allogeneic bone marrow transplantation for lysosomal storage diseases. The European Group for Bone Marrow Transplantation. *Lancet* **345**(8962), p. 1398–402 (1995).
10. Vellodi, A. *et al.* Bone marrow transplantation for mucopolysaccharidosis type I: experience of two British centres. *Arch Dis Child* **76**(2), p. 92–9 (1997).
11. Gullingsrud, E. O., W. Krivit & C. G. Summers, Ocular abnormalities in the mucopolysaccharidoses after bone marrow transplantation. Longer follow-up. *Ophthalmology* **105**(6), p. 1099–105 (1998).
12. Souillet, G. *et al.* Outcome of 27 patients with Hurler's syndrome transplanted from either related or unrelated haematopoietic stem cell sources. *Bone Marrow Transplant* **31**(12), p. 1105–17 (2003).
13. Sharma, A. *et al.* AAV serotype influences gene transfer in corneal stroma *in vivo*. *Exp Eye Res* **91**(3), p. 440–8 (2010).
14. Hippert, C. *et al.* Corneal transduction by intra-stromal injection of AAV vectors *in vivo* in the mouse and *ex vivo* in human explants. *PLoS One* **7**(4), p. e35318 (2012).
15. Mohan, R. R. *et al.* Targeted decorin gene therapy delivered with adeno-associated virus effectively retards corneal neovascularization *in vivo*. *PLoS One* **6**(10), p. e26432 (2011).
16. Grieger, J. C. & R. J. Samulski, Adeno-associated virus as a gene therapy vector: vector development, production and clinical applications. *Adv Biochem Eng Biotechnol* **99**, p. 119–45 (2005).
17. Simpson, D. A. *et al.* Telomerase expression is sufficient for chromosomal integrity in cells lacking p53 dependent G1 checkpoint function. *J Carcinog* **4**, p. 18 (2005).
18. Shapiro, E. G. *et al.* Neuropsychological outcomes of several storage diseases with and without bone marrow transplantation. *J Inherit Metab Dis* **18**(4), p. 413–29 (1995).
19. Whitley, C. B. *et al.* Long-term outcome of Hurler syndrome following bone marrow transplantation. *Am J Med Genet* **46**(2), p. 209–18 (1993).
20. Prasad, V. K. *et al.* Unrelated donor umbilical cord blood transplantation for inherited metabolic disorders in 159 pediatric patients from a single center: influence of cellular composition of the graft on transplantation outcomes. *Blood* **112**(7), p. 2979–89 (2008).
21. Boelens, J. J. *et al.* Outcomes of transplantation of unrelated cord blood in children with malignant and non-malignant diseases: an Utrecht-Prague collaborative study. *Bone Marrow Transplant* **43**(8), p. 655–7 (2009).
22. Summers, C. G. *et al.* Ocular changes in the mucopolysaccharidoses after bone marrow transplantation. A preliminary report. *Ophthalmology* **96**(7), p. 977–84; discussion 984–5 (1989).
23. Traas, A. M. *et al.* Correction of clinical manifestations of canine mucopolysaccharidosis I with neonatal retroviral vector gene therapy. *Mol Ther* **15**(8), p. 1423–31 (2007).
24. Hinderer, C. *et al.* Neonatal Systemic AAV Induces Tolerance to CNS Gene Therapy in MPS I Dogs and Nonhuman Primates. *Mol Ther* **23**(8), p. 1298–307 (2015).
25. Grieger, J. C., V. W. Choi & R. J. Samulski, Production and characterization of adeno-associated viral vectors. *Nat Protoc* **1**(3), p. 1412–28 (2006).
26. Aronovich, E. L. *et al.* Systemic correction of storage disease in MPS I NOD/SCID mice using the sleeping beauty transposon system. *Mol Ther* **17**(7), p. 1136–44 (2009).
27. Garcia-Rivera, M. F. *et al.* Characterization of an immunodeficient mouse model of mucopolysaccharidosis type I suitable for preclinical testing of human stem cell and gene therapy. *Brain Res Bull* **74**(6), p. 429–38 (2007).

## Acknowledgements

We kindly thank Dr. Elena L. Aronovich, at University of Minnesota for providing the pT2/IDUA//Ub-SB11 plasmid, which allowed comparison between wild type and optimized IDUA cDNA sequences. This work was supported by NCTRACs, the UPENN rare disease endowment, and the NIH (RO1AI072176-06A1, RO1AR064369-01A1, T32 5T32HL007149-39). Funding was also provided in part through a departmental Unrestricted Grant from Research to Prevent Blindness, New York, NY, USA. We would also like to thank Miracles in Sight for providing human tissue for these experiments.

## Author Contributions

M.V., T.L., W.B., K.W., G. M., N.C., B.G. and M.L.H. performed the experiments. All authors contributed to manuscript preparation. A.A., B.G., J.K., R.J.S. and M.L.H. designed the experiments to be tested herein.

## Additional Information

**Supplementary information** accompanies this paper at <http://www.nature.com/srep>

**Competing financial interests:** R. Jude Samulski is the founder and a shareholder at Asklepios BioPharmaceutical. He receives research support through the University of North Carolina from Asklepios.

BioPharmaceutical. He holds patents that have been licensed by UNC to Asklepios. Biopharmaceutical, for which he receives royalties. He has consulted for Baxter Healthcare and has received payment for speaking. Matthew Hirsch has disclosed AAV8G9-optIDUA to the University of North Carolina.

**How to cite this article:** Vance, M. *et al.* AAV Gene Therapy for MPS1-associated Corneal Blindness. *Sci. Rep.* **6**, 22131; doi: 10.1038/srep22131 (2016).



This work is licensed under a Creative Commons Attribution 4.0 International License. The images or other third party material in this article are included in the article's Creative Commons license, unless indicated otherwise in the credit line; if the material is not included under the Creative Commons license, users will need to obtain permission from the license holder to reproduce the material. To view a copy of this license, visit <http://creativecommons.org/licenses/by/4.0/>